*Physicochem. Probl. Miner. Process., 54(2), 2018, 496-504*

http://www.journalssystem.com/ppmp/

Physicochemical Problems of Mineral Processing

ISSN 1643-1049


*Received August 3, 2017; reviewed; accepted September 28, 2017*

# Adsorption behaviors of typical aromatic pollutants in biologically treated coking wastewater on powdered coal

**Hao Sun [1,2], Yongtian Wang [1,2], Yue Bian [1,2], Xin He [1], Guosheng Li [1,2]**

[1] School of Chemical Engineering and Technology, China University of Mining &Technology, Xuzhou221116, Jiangsu, China

[2] Chinese National Engineering Research Center of Coal Preparation and Purification, China University of Mining &Technology, Xuzhou 221116, Jiangsu, China

Corresponding author: wytcumtkj@126.com (Yongtian Wang)

**Abstract:** The raw coal was utilized as adsorbent based on its remarkable adsorption ability of coal slime to organic compounds in the flotation process. This paper mainly investigates adsorption behaviors of benzpyrole (BZP), pyrrole (PR) and benzoic acid (BA) on powdered coal (PC). In the monocomponent solution, the removal efficiencies of BZP, PR and BA reached 85.23%, 55.02% and 24.84% at PC dosage of 20 g/dm$^3$. Adsorption behaviors of three pollutants fitted perfectly to the pseudo-second order kinetics model and liquid film diffusion occupied the largest proportion in rate-limiting step according to the diffusion rates. Furthermore, the influences of pH on adsorption behaviors and competitive adsorption mechanism of three pollutants were also reported.

***Keywords:*** *aromatic pollutants, wastewater treatment, adsorption affinity, competitive adsorption*

## 1. Introduction

Multifarious poisonous aromatic contaminant in the coking wastewater possess stable chemical structures and strong biological toxicity, such as benzpyrole, quinoline, biphenyl and naphthalene (Ania et al., 2007; Zhang et al., 2010; Zhang et al., 2013), which are difficult to degrade and produced a huge impact on the environment. Given the limitations of biochemical technology at present, the concentration of organic matters remains high in above 90% of coking wastewater after the biological treatment (AO, AAO, SBR) procedures. Excessive pollutants are transferred to the atmosphere or water system through the wet quenching process, which made a great hazard to the ecological environment (Choubert et al., 2011; Verlicchi et al., 2012). Therefore, the advanced treatment technologies are needed to recycle well treated effluents for environmental or beneficial reuse purposes. Carbon adsorption is widely used for removing organic matters from wastewater because it is less operationally and consumes less energy than other methods such as oxidation, reverse osmosis and micro-electrolysis (Xing et al., 2015; Li et al., 2016).

Carbon-based adsorbents have been extensively studied as a promising adsorbent for removing organic pollutants from the aqueous solution (Altmann et al., 2014). The utilization of activated carbon has achieved the purification of wastewater due to its huge specific surface area and developed porous structure (Zhang et al., 2010; Fu et al., 2012; Sun et al., 2016). Studies showed that activated carbon displayed efficient removal ability of aromatic protein-like matters which contributed mostly to the remaining acute toxicity of the biologically treated effluents (Ma et al., 2016), but the specific pollutant was not mentioned. Ren et al (2013) investigated the adsorption of phenol, aniline and n-heptane from biologically treated coking wastewater on powdered activated carbon; results showed that long-chain alkanes, benzoic, halogenated and phenolic compounds were adsorbed well under acidic condition, while amines were adsorbed well under alkaline condition.

In the coal slime flotation process, coal particles show strong adsorption of organic hydrocarbon. Based on this, a novel technology proposed the application of coking raw materials in purification of

http://dx.doi.org/10.5277/ppmp1850

coking wastewater. Previous research also showed that the removal efficiencies of COD (chemical oxygen demand) and clarity at the PC dosage of 40 g/dm$^3$ and pH value of 2 reached to 75.66% and 90.22% respectively (Gao et al., 2015). The used PC can be recycled to the coking or heating system, which put an end to the secondary transfer of pollutants and extracted more potential value of coal. Xu et al (2016) employed Lignite, coking coal and anthracite as adsorbents to remove quinolone from coking wastewater and the process of quinoline adsorption onto three kinds of coal follows pseudo-second-order rate kinetics. Moreover, it was found that the humic substance was easier to remove than other substances such as proteins, carbohydrates, fluorescence aromatic protein and SMPs by brown coal from the wastewater (Mohammad et al., 2017). Despite various researches conducted on coal adsorption, there have been no documented studies found on competitive adsorption on coal among the aromatic pollutants.

As the typical aromatic pollutants, pyrrole (PR), benzpyrole (BZP) and benzoic acid(BA) represent micro molecules with heterocyclic structure, fused-heterocycle and aromatic carboxylic acid, respectively. In addition to the long chain alkanes, they are the major contributors to the COD of bio-treated coking wastewater. The molecular diameters of these three contaminants are 4.35Å, 6.91Å and 6.74 Å separately. As mentioned above, this study aims to investigate and explain the microcosmic adsorption behaviors of different aromatic pollutants on PC. Our results can provide efficient data support for target pollutant removal and coking wastewater advanced treatment in the future.

## 2. Materials and methods

The coal sample from Shenmu County in Shanxi Province was pulverized into fine particles which pass through 200 mesh sieve accounted for 85% of total with a pendulum jaw crusher and a ball mill. Three typical organic pollutants (pyrrole, benzpyrole, and benzoic acid) with analytical grade and purity above 99.7% were purchased from Sinopharm Chemical Reagent Co., Ltd, China.

An automated specific surface area analyzer (BELSORP-max, MicrotracBEL, JAPAN) was applied to characterize the particle structure. The specific surface area($S_{BET}$) and pore volume distributions were calculated by the method reported by Barrett et al (Barrett et al., 1951). The surface compositions, micro-topography and chemical composition of Shenmu coal were analyzed using X-Ray Photoelectron Spectrometer (ESCALAB 250Xi, Thermo Fisher, USA) and X-ray fluorite spectrometer (S8 TIGER, Bruker, Germany) respectively.

Static adsorption tests were conducted in sealed conical flasks with various amounts of adsorbent and 100 cm$^3$ pollutants contained solution. All tests were performed in a thermostatic shaker bath under a selected temperature for the needed time. All the mixtures had been centrifuged at 3000 rpm for 10 min after adsorption equilibrium, and the supernate were further detected afterwards. In the competitive adsorption test, the pickled powdered coal (PPC) was employed to avoid the acid effect on the physical structure of coal. The solute concentration of supernate was respectively detected by UV-visible spectrophotometer (UV-4208S, Unico, China) at 230 nm, 237 nm and 275 nm based on the full spectrum scan of single pollutant. Each test was repeated three times and all duplicates varied by less than 3%.

## 3. Results and discussion

### 3.1 Characterization of PC

The physicochemical properties analysis results (Table 1) shows that PC can be used as a natural high quality adsorbent. It is appropriate for PC to recycle to the heating system after adsorption process because of its high organic composition content and calorific value. XRD analysis indicates that the inorganic components in Shenmu long-flame coal mainly include calcite, quartz and few clay minerals, which is advantageous to the subsequent solid-liquid separation process. According to the proportion of mesopore volume (57.27%) among the total volume in BET analysis, PC could be judged as a mesoporous material.

### 3.2 Adsorption kinetics

Kinetics information of PR, BZP and BA adsorption is required to determine the contact time for their batch removal tests. The pollutants concentration is 30 mg/dm$^3$ and the aqueous sample was taken at

pre-set time interval. All tests were performed at 20 °C, adsorbent dosage of 20 g/dm³ and the pH of the solution maintains at 7.1. Kinetics data of different pollutants are presented in Fig.1, the remove rate ($\gamma$) of pollutants increase dramatically in the first 50 min. Then the equilibrium of all adsorbates is all gradually achieved within 240 min. Fig.1 also shows that BZP has larger equilibrium γ than PR and BA. BZP got a γ of 85.23%, while PR and BA got 55.02% and 24.84% respectively.

Table 1. Physical and chemical properties of PC

| Chemical composition (%) | Value | Industrial analysis (%) | Value | BET analysis | Value |
|---|---|---|---|---|---|
| CaO | 49.8 | $M_{ad}$ | 6.01 | $S_{BET}$(m²/g) | 7.64 |
| $SiO_2$ | 24.5 | $A_d$ | 5.15 | $V_T$(cm³/g) | 0.0215 |
| $Al_2O_3$ | 9.54 | $V_{daf}$ | 37.5 | $V_{mes}$(cm³/g) | 0.0123 |
| MgO | 1.02 | Fcd | 59.3 | $V_{mic}$(cm³/g) | 0.0092 |
| $Fe_2O_3$ | 5.85 | $Q_d$(MJ/kg) | 23.6 | A (nm) | 3.79 |
| $Na_2O$ | 1.75 | | | | |
| Others | 7.54 | | | | |

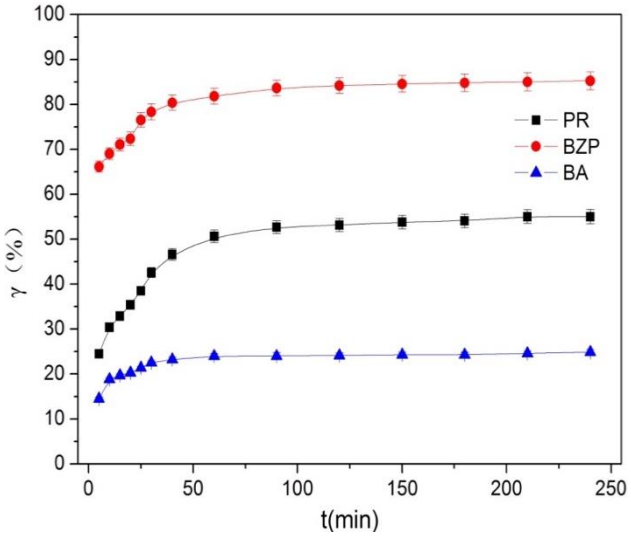


Fig. 1. Adsorption kinetics of PR, BZP and BA on PC (initial concentration 30 mg/dm³; adsorbent dosage 20 g/dm³; natural pH 7.1; temperature 20 °C)

In this research, three kinetic models are applied to analyze the adsorption process includes Pseudo-first-order kinetics model, Pseudo-second-order kinetics model and Weber-Morris intra-particle diffusion model describe the different diffusion mechanisms respectively in adsorption process. They are given by the following equations (Lorenc-Grabowska et al., 2013; Sun et al., 2014):

$$\ln(q_e - q_t) = \ln q_e - \frac{k_1 t}{2.303} \quad (1)$$

$$\frac{t}{q_t} = \frac{1}{k_2 q_e^2} + \frac{t}{q_e} \quad (2)$$

$$q_t = k_{ip} t^{1/2} + C \quad (3)$$

where $q_e$ and $q_t$ (mg/g) stand for the adsorption capacities at equilibrium and a given time (min), respectively, $k_1$ (min$^{-1}$) and $k_2$ [g/(mg min)] are known as the rate constants of the pseudo-first-order and pseudo-second-order models, respectively and $k_{ip}$ [mg/(g min$^{0.5}$)] is the diffusion rate constant of intra-particle diffusion model, while $C$ represents the boundary layer thickness.

The adsorption data of three organic matters were fitted to kinetic models and Table 2 list the kinetics models parameters. The pseudo-second-order model possesses higher correlation coefficients, and the experimental $q_e$ values are even closer to the theoretically measured values, which indicated the pseudo-second-order model was suitable for describing the adsorption process. The rate constant $k_2$ followed the order of BZP>PR>BA.

Table 2. Kinetics parameters during the sorption of PR, BZP and BA (Initial concentration 30 mg/dm$^3$; adsorbent dosage 20 g/dm$^3$; natural pH 7.1; temperature 293 K)

| Kinetic models | Constants | PR | BZP | BA |
|---|---|---|---|---|
| Pseudo-first-order | $q_{e1}$ (mg/g) | 0.4486 | 0.5641 | 0.2153 |
| | $k_1$ (min$^{-1}$) | 0.0488 | 0.0783 | 0.0403 |
| | $R^2$ | 0.8574 | 0.9068 | 0.9463 |
| | $q_e$ | 0.5502 | 1.2751 | 0.3726 |
| pseudo-second-order | $q_{e2}$ (mg/g) | 0.5993 | 1.3011 | 0.4904 |
| | $k_2$ [g/(mg min)] | 0.1382 | 0.2205 | 0.2077 |
| | $R^2$ | 0.9438 | 0.9934 | 0.9555 |
| intra-particle diffusion | $k_{ip1}$ mg/(g min$^{0.5}$) | 0.0443 | 0.0559 | 0.0485 |
| | $C_1$ (mg/g) | 0.1542 | 0.8578 | 0.1150 |
| | $R^2$ | 0.9865 | 0.9619 | 0.9174 |
| | $k_{ip2}$ mg/(g min$^{0.5}$) | 0.0128 | 0.0127 | 0.0112 |
| | $C_2$ (mg/g) | 0.4071 | 1.1282 | 0.2395 |
| | $R^2$ | 0.9998 | 0.9676 | 0.8791 |
| | $k_{ip3}$ mg/(g min$^{0.5}$) | 0.0061 | 0.0032 | 0.0020 |
| | $C_3$ (mg/g) | 0.4586 | 1.2296 | 0.3401 |
| | $R^2$ | 0.9561 | 0.9988 | 0.8954 |

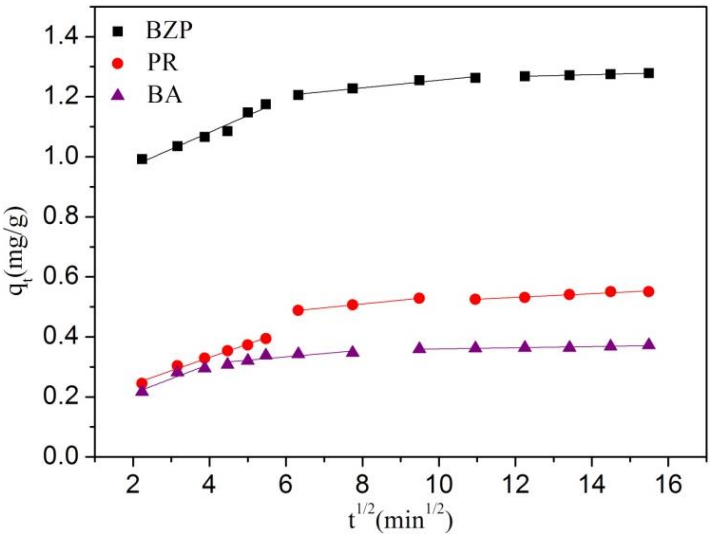


Fig. 2. Intra-particle diffusion model of PR, BZP and BA adsorption by PC

Fig. 2 demonstrates that the adsorption process of all organic matters present a multi-linearity and fitting lines disjointed to zero point implying that the adsorption rate is dominated by multiple mechanisms including internal diffusion. It proved that three stages occurred in the adsorption process containing liquid film diffusion, intra-particle diffusion and sorption in micro pore. The constant C which reflects the thickness of the boundary layer indicates that the liquid film diffusion contributed most to the adsorption rate of BZP. The related parameters $k_{ip1}$ show that BZP has the maximum liquid film diffusion rate which indicates that BZP sorption was the fastest in equilibrium reaching. Besides, BA is the most difficult pollutant to remove which has been found in other studies (Lladó et al., 2017).

Compared to other adsorbents (biochar, $S_{BET}$ = 745.3 m$^2$/g, 68.5 mg/g for nitroaniline and 5.98 mg/g for BA), PC ($S_{BET}$ = 7.64 m$^2$/g, 1.30 mg/g for BZP and 0.49 mg/g for BA) get lower adsorption capacity under the same conditions (Akila et al., 2017). However, PC (0.17 mg/m$^2$ for BZP and 0.06

mg/m² for BA) has higher adsorption capacity per unit surface area than biochar (0.092 mg/m² for nitroaniline and 0.01 mg/m² for BA) does. Based on this, we believe that PC achieves higher surface area utilization ratio than other adsorbents and it is economical because of saving the cost on adsorbent activation process.

### 3.3 Effect of pH

Adsorption experiments of three organic pollutants were completed under different pH values. The results show the removal efficiency of all typical pollutants increase with the decrease of PH. When the pH values decreased from 7.1 to 2.0, the remove efficiency of PR, BZP and BA increase from 39.44% to 63.63%, 78.34% to 91.14%, and 22.54% to 43.69% respectively. It is obvious that the initial pH plays a significant role in adsorption process, which can produce a noticeable effect on the physicochemical properties of pollutants molecules, texture structure of adsorbent and solution environment. Structural differences between the PC and PPC are systematically investigated as follows.

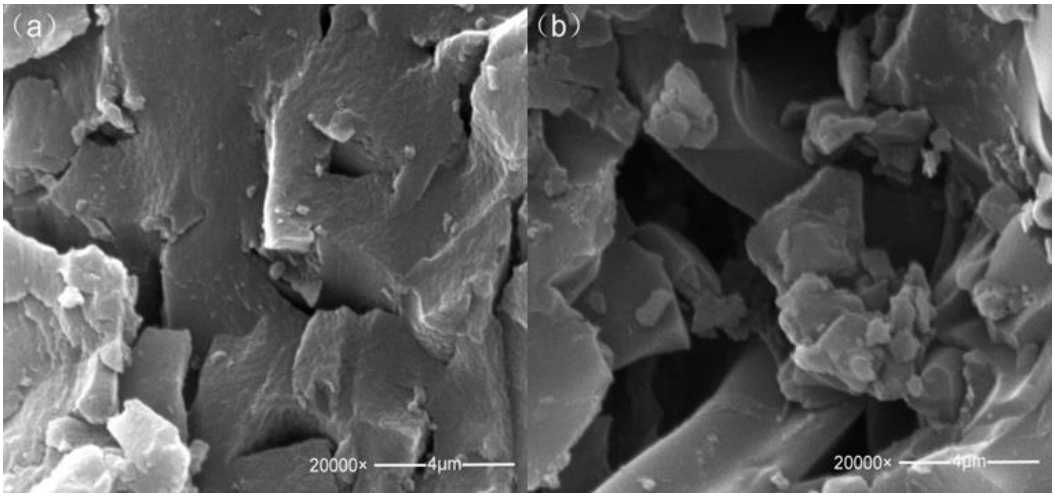


Fig. 3. SEM micrograph of (a)PC and (b)PPC

As shown by the SEM images (Fig. 3), the pickling step induces the growth of porosity on PC. According to the BET analysis, the SBET and VT values increase to 10.70 m²/g and 0.0246 cm³/g, respectively. The average pore size drops from 3.79 nm to 3.60 nm which are mainly caused by the increase in micropore content.

Fig. 4 presents the XPS peak-differentiation-imitating spectra of PC and PPC. It is well known that the C1s peak can be categorized into four components (Sánchez-Sánchez et al., 2014), Peak 1 (283.9 eV), Peak 2 (284.6 eV), Peak 3(286.2 eV) and Peak 4(287.0 eV) are regarded as carbon-hydrogen bond (C-H), the pure graphitic or amorphous C-C, the C-O (phenols, ethers, anhydrides) and C-N respectively. Comparing Fig.4a with Fig.4b, the pickling step alters C-C and C-H contents from 64.01% to 64.92% and 13.19% to 16.39%, which is beneficial to the adsorption process because of the exposure of hydrophobic surfaces. The Boehm's titration (Oickle et al., 2010) results show that the content of the acid group on the surface increases from 0.0633 nmol/dm³ to 0.0802 nmol/dm³ after pickling. A consensus is that basic groups are prone to adsorb nonpolar molecules, while the acidic groups are prone to adsorb polar molecules (Leng et al., 2015).

After acid treatment, the specific surface area of PC increases with a certain amount of mineral dissolution, while the dissolved minerals transfer to the liquid phase in the form of inorganic ions. With the decrease of pH value, the amount of dissolved ions increased. The detection result of pickling solution by ion chromatography indicates that the dissolved ions mainly include $Ca^{2+}$, $Mg^{2+}$ and $Fe^{3+}$, etc. The effect of initial $Ca^{2+}$ concentrations on removal efficiency are also studied (Fig.5). It shows that the presence of inorganic ions and a large amount of $H^{+}$ significantly reduce the electronegativity of coal surface and results in the decrease of electrostatic repulsion between the

adsorbents and the adsorbates in bulk phase, which make easier adsorption of contaminants than without inorganic ions.

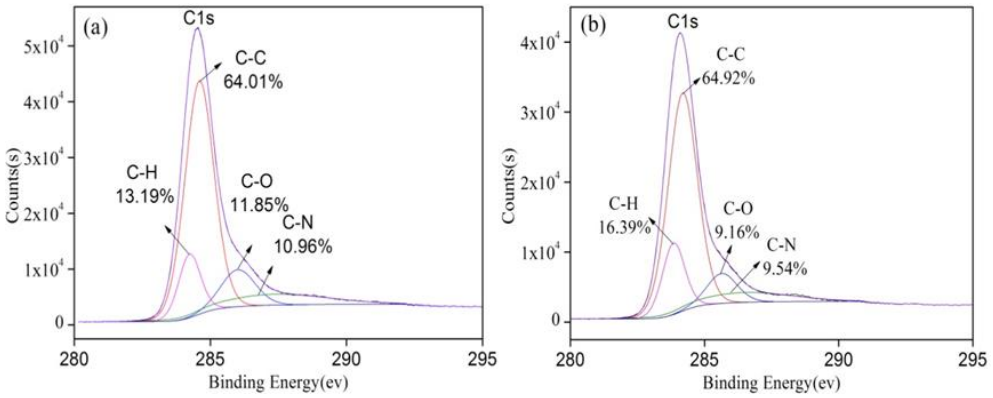


Fig. 4. High resolution scans of C1s for (a) PC and (b) PPC

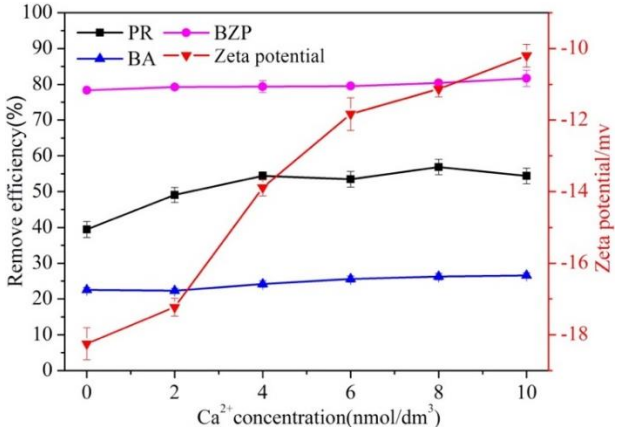


Fig. 5. Zeta potential of PC in different $Ca^{2+}$ concentration and its influence on pollutants removal (Initial concentration 30 mg/dm$^3$; adsorbent dosage 20 g/dm$^3$; natural pH 7.1; temperature 293 K)

In addition, BA molecules show different electrical properties and existence state under different pH conditions (Fig. 6). With increasing pH value, the electronegativity of BA continually increases due to the deprotonating effect. BA exists mainly in the form of ions at pH = 7. Meanwhile, the weak adsorption intensity of BA on PC leads to the lower removal efficiency. However, above 99% of BA exists in molecular form at pH = 2 and the reduction of hydrogen bonding interaction between the hydroxyl group and water molecules causes the enhanced adsorption force and improved removal efficiency.

### 3.4 Competitive adsorption behaviors

As Fig. 7a shows, the existence of PR has a minor influence on the adsorption behavior of BZP, which indicates the weak competition between BZP and PR. The adsorption capacity of PR significantly falls at first and then slightly increases with the growth of BZP concentration. This may be explained by the combination of PR and adsorbed BZP through π-π interaction that forms a multilayer adsorption.
Figs. 7b and 7c present the adsorption isotherms of BZP and PR in the presence of dissociated BA (DBA) and molecular BA (MBA) respectively. The adsorption capacity of BZP and PR are less influenced by the concentration changes of DBA compared with MBA. In addition, the competitive effect of BZP strongly inhibits the DBA adsorption performance, which demonstrates the competitive advantage of BZP for active sites. However, the adsorption capacity of BZP and PR decreases gradually with growing concentration of MBA, while the increased 1/n indicates that the uptake of BZP becomes more difficult due to the weak adsorption intensity of DBA on PPC. The higher adsorption intensity of MBA leads to the reduction of BZP uptake with the increasing MBA

concentration. Adsorption affinity of BZP reduces due to the hydrophobic enhancement of PPC caused by carboxyl groups of the adsorbed MBA, while the uptake of PR is less affected because it could enter the micropore with smaller molecular size than other adsorbates.

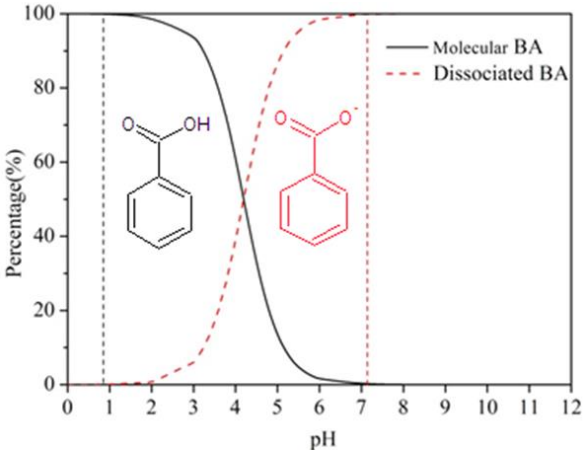


Fig. 6. Relative proportion of BA species under different pH

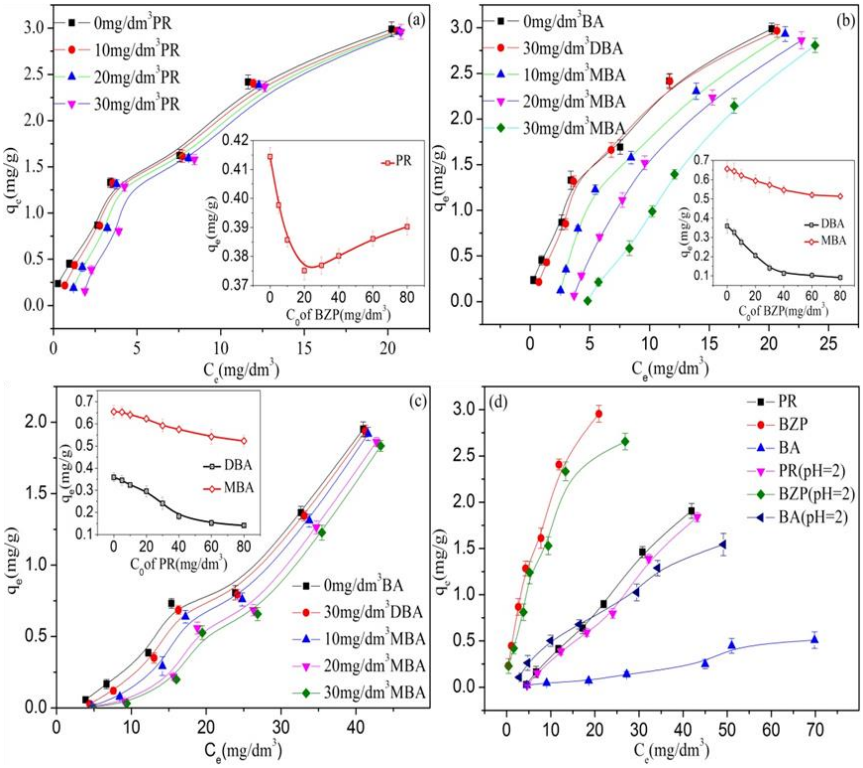


Fig. 7. Competitive adsorption isotherms of (a) BZP in the presence of PR(b) BZP in the presence of BA (c) PR in the presence of BA (d) tri-component

Fig. 7d gives the competitive adsorption isotherms of three solutes. According to the results, PR, BZP and BA compete directly with each other for the active sites. The final adsorption capacities of different typical contaminants are determined by physisorption contains hydrogen bond, hydrophobic interaction, electrostatic attraction and π-π interaction. The strongest hydrophobic interaction between BZP and the PPC resulted in maximum adsorption capacity of BZP. It is also proved the preferential adsorption for the fused-heterocycle molecules compared to micro heterocyclic molecules and aromatic carboxylic acid on PPC.

## 4. Conclusions

Powdered coal was obtained from coking plant and employed to remove the typical aromatic pollutants of biologically treated coking wastewater. Adsorption intensity of typical pollutants by PC followed the order of BZP>PR>BA. Low pH value promoted the adsorption process via extending organic surfaces of PC (77.20% to 81.31% for C-C and C-H), minimizing the electrostatic repulsion between PC surface and organic matters and changing the pollutants forms (dissociated BA to molecular BA).

Based on the competitive adsorption isotherms, the adsorbed fused-heterocycle matters could strongly inhabit the aromatic carboxylic acid adsorption via competitive effect. It was concluded that PC adsorption process could further eliminate the residual pollutants of bio-treated effluent, but most of aromatic carboxylic acid compounds still remained in the effluent. Above all, in order to guarantee the deep purification of bio-treated cooking wastewater, the targeted removal of aromatic carboxylic acid should have gotten more attention.

**Acknowledgements**

This research was supported by the National Nature Science Foundation of China (No. 51504254, 51274198), the Fundamental Research Funds for the Central Universities of China (No. 2015XKMS039) and the Natural Science Foundation of Jiangsu Province (BK20150192) for which the authors express their appreciation.

**References**

ALTMANN, J., RUHL, A.S., ZIETZSCHMANN, F., JEKEL, M., 2014. *Direct comparison of ozonation and adsorption onto powdered activated carbon for micropollutant removal in advanced wastewater treatment*. Water Res., 55, 185-193.

ANIA, C.O., CABAL, B., PEVIDA, C., ARENILLAS, A., PARRA, J.B., RUBIERA, F., PIS, J.J., 2007. *Removal of naphthalene from aqueous solution on chemically modified activated carbons*. Water Res., 41, 333-340.

AKILA, G.K., OLIVIA, A.T., MORGAN, L.C., LINDSEY, B.R., CHARLES, U.P., RENEL, A., TODD, E.M., 2017. *Rapid removal of salicylic acid, 4-nitroaniline, benzoic acid and phthalic acid from wastewater using magnetized fast pyrolysis biochar from waste Douglas fir*. Chem. Eng. J., 319, 75-88.

BARRETT, E.P., JOYNER, L.G., HALENDA, P.P., 1951. *The Determination of Pore Volume and Area Distributions in Porous Substances. I. Computations from Nitrogen Isotherms*. J. Am. Chem. Soc., 73, 373-380.

CHOUBERT, J.M., RUEL, S.M., GSPERANZA, M., BUDZINSKI, H., MIEGE, C., LAGARRIGUE, C., COQUERY, M., 2011. *Limiting the emissions of micro-pollutants: what efficiency can we expect from wastewater treatment plants*? Water Sci. Technol., 63, 57-65.

FU, D., ZHANG, Y., LV, F., CHU, P., SHANG, J., 2012. *Removal of organic materials from TNT red water by Bamboo Charcoal adsorption*. Chem. Eng. J., 193, 39-49.

GAO, L., LI, S., WANG, Y., SUN, H., 2015. *Organic pollution removal from coke plant wastewater using coking coal*. Water Sci. Technol., 72, 158-163.

LENG, L., YUAN, X., ZENG, G., SHAO, J., CHEN, X., WU, Z., WANG, H., PENG, X., 2015. *Surface characterization of rice husk bio-char produced by liquefaction and application for cationic dye (Malachite green) adsorption*. Fuel, 155, 77-85.

LI, J., WU, J., SUN, H., CHENG, F., LIU, Y., 2016. *Advanced treatment of biologically treated coking wastewater by membrane distillation coupled with pre-coagulation*. Desalination, 380, 43-51.

LLADÓ, J., GIL, R.R., LAO-LUQUE, C., SOLÉ-SARDANS, M., FUENTE, E., RUIZ, B., 2017. *Highly microporous activated carbons derived from biocollagenic wastes of the leather industry as adsorbents of aromatic organic pollutants in water*. J. Environ. Chem. Eng., 5, 2090-2100.

LORENC-GRABOWSKA, E., GRYGLEWICZ, G., DIEZ, M.A., 2013. *Kinetics and equilibrium study of phenol adsorption on nitrogen-enriched activated carbons*. Fuel, 114, 235-243.

MA, D.H., LIU, C., ZHU, X.B, LIU, R., CHEN, L.J., 2016. *Acute toxicity and chemical evaluation of coking wastewater under biological and advanced physicochemical treatment processes*. Environ. Sci. Pollut. Res., 23, 18343-18352.

MOHAMMAD, A.N., FARZAD, M., BIPLOB, K.P., MAAZUZA O., TIM, M., MUHAMMED A.B., 2017. *Application of Victorian brown coal for removal of ammonium and organics from wastewater*. Environ. Technol., DOI: 10.1080/09593330.2017.1319424.

OICKLE, A. M., GOERTZEN, S. L., HOPPER, K. R., ABDALLA, Y. O., ANDREAS, H. A., 2010. *Standardization of the Boehm titration: Part II. Method of agitation, effect of filtering and dilute titrant*. Carbon, 48, 3313-3322.

REN, Y., LI, T., WEI, C.H., 2013. *Competitive Adsorption Between Phenol, Aniline and n-Heptane in Tailrace Coking Wastewater*. Water Air Soil Pollut., 224, 1365-1375.

SÁNCHEZ-SÁNCHEZ, A., SUÁREZ-GARCÍA, F., MARTINET-ALONSO, A., TASCON, J., 2014. *Aromatic polyamides as new precursors of nitrogen and oxygen-doped ordered mesoporous carbons*. Carbon, 70, 119-129.

SUN, W., QU, Y., YU, Q., NI, J., 2008. *Adsorption of organic pollutants from coking and papermaking wastewaters by bottom ash*. J. Hazard. Mater., 154, 595-601.

SUN, Y., YUE, Q., GAO, B., GAO, Y., XU, X., LI, Q., WANG, Y., 2014. *Adsorption and cosorption of ciprofloxacin and Ni(II) on activated carbon-mechanism study*. J. Taiwan Institute Chem. Eng., 45, 681-688.

VERLICCHI, P., AUKIDY, M. A. I., ZAMBELLO, E., 2012. *Occurrence of pharmaceutical compounds in urban wastewater: removal, mass load and environmental risk after a secondary treatment*. Sci. Total Environ., 429, 123-155.

XING, R., ZHEN, Z., WEN, D., 2015. *Comparison between UV and VUV photolysis for the pre-and post-treatment of coking wastewater*. J. Environ. Sci., 29, 45-50.

XU, H.X.; HUANG, G.; LI, X.B. GAO, L.H.; Wang Y.T., 2016. *Removal of quinoline from aqueous solutions by lignite, coking coal and anthracite: Adsorption Isotherms and thermodynamics*. Physicochem. Probl. Miner. Process., 52, 214-227.

ZHANG, H.Q., YE, C.S., YANG, F., ZHANG, X., YANG, H., LIU, G.R., 2013. *Analysis of Organic Pollutants from Biologically Treated Coking Wastewater in a Multiple Barrier Method*. Adv. Mater. Res., 641, 165-168.

ZHANG, M., ZHAO, Q., BAI, X., YE, Z., 2010. *Adsorption of organic pollutants from coking wastewater by activated coke*. Colloids Surf. A, 362, 140-146.

ZHANG, S., SHAO, T., KOSE, H. S., KARANFIL, T., 2010. *Adsorption of aromatic compounds by carbonaceous adsorbents: a comparative study on granular activated carbon, activated carbonfiber, and carbon nanotubes*. Environ. Sci. Technol., 44, 6377-6383.